




# Enhanced thermal conductivity of diamond/aluminum composites through tuning diamond particle dispersion

Zhanqiu Tan<sup>1</sup>, Ding-Bang Xiong<sup>1</sup>, Genlian Fan<sup>1,\*</sup>, Zhizhong Chen<sup>1</sup>, Qiang Guo<sup>1</sup>, Cuiping Guo<sup>1</sup>, Gang Ji<sup>2</sup>, Zhiqiang Li<sup>1,\*</sup> , and Di Zhang<sup>1</sup>

<sup>1</sup> State Key Laboratory of Metal Matrix Composites, School of Materials Science and Engineering, Shanghai Jiao Tong University, Shanghai 200240, China

<sup>2</sup> Unité Matériaux et Transformations (UMET), CNRS, UMR 8207, Université Lille 1, 59655 Villeneuve d'Ascq, France

Received: 11 October 2017

Accepted: 11 January 2018

Published online:  
24 January 2018

© Springer Science+Business  
Media, LLC, part of Springer  
Nature 2018

## ABSTRACT

Diamond/aluminum (Dia/Al) composites were fabricated by powder metallurgy using starting Al powders of different size. Effect of matrix-to-reinforcement particle size ratio (PSR) on diamond particle dispersion was revealed, and higher thermal conductivity of Dia/Al composites with a certain volume fraction was achieved by changing PSR. The results indicated that, with PSR increasing from 0.225 to 0.9, diamond particles tended to show a connecting dispersion and the thermal conductivity of 40 and 50 vol.% Dia/Al composites increased by 21% (from 389 to 472 W/mK) and by 42% (from 442 to 628 W/mK), respectively. The underlying cause was discussed from the point of the coordination number of Al powders around diamond particles. This study supplies a new idea to improve thermal conductivity of Dia/Al composites by tuning particle dispersion for the first time, which is also applicable to other metal matrix composites.

## Introduction

Thermal management has become one of the most challenging issues in electronic industry because of the ever increasing power density. Efficient heat removal urgently requires novel high thermal conductive materials used as heat sink and/or substrate to improve the reliability and lifetime of electronic components [1–4]. Metal matrix composites (MMCs), especially incorporating highly conductive diamond

particles, have drawn much more attentions than ever before, due to their high thermal conductivity (TC) and tailorable coefficient of thermal expansion (CTE), which is expected to positively contribute to heat dissipation and to minimize thermal stress between the electronic components and thermal substrate [5, 6].

To achieve higher TC in MMCs, four strategies were generally considered: (a) the selection of high thermal conductive metal matrix, such as Al, Cu and

Address correspondence to E-mail: fangenlian@sjtu.edu.cn; lizhq@sjtu.edu.cn

Ag [1, 7]; (b) large diamond particles (even 300–600  $\mu\text{m}$  in size [5, 8–10]) with high purity and regular polyhedral shapes [8, 11–13]; (c) high volume fraction of diamond particles incorporated in metal matrix (61–74 vol.%), e.g., by tapping of bimodal particle mixtures [5, 9, 14–16]; (d) subtle interface engineering between the diamond particles and the metal matrix, e.g., by elaborately controlling interface diffusion and reaction via processing temperature and time optimization [11, 17–20], or by introducing an additional carbide layer via diamond surface metallization or matrix alloying, such as Ti, W, Cr, B and Si carbide forming elements [5, 6, 21–27].

However, it is much limited to choose diamond particles with rather large size and/or high purity, while it is also infeasible to incorporate diamond particles with volume fraction higher than 70 vol.%, which may deteriorate the formability, consolidation and mechanical performances of these composites. For this consideration, it is essential to explore alternative approaches to higher TC of MMCs with certain volume fraction of the selected diamond particles. On the other hand, the tailorability of particle dispersion in matrix instead of the homogeneous dispersion has been not paid enough attentions so far [28, 29], which may be especially effective in functional property enhancement for composites with high phase contrast between reinforcement and matrix. Typically, it was reported that electrical conductivity of the conductive metallic or carbonous particulates reinforced dielectric polymers was remarkably enhanced by increasing the connected particle dispersion [30]. And in most cases, the concept of thermal resistance can analogize an electrical one [17, 31] and indicates the potential effect of particle dispersion on the TC of MMCs, which is still an open topic to be discussed till now.

As one of the most promising candidates for thermal management applications, diamond/Al (Dia/Al for short hereafter) composite shows the potential combination of high TC, tailorable CTE and light weight, especially with TC much higher than that of the commercially applied SiC/Al counterparts though accompanying several times higher cost. In this work, 40–50 vol.% Dia/Al composites were fabricated by powder metallurgy (PM) to study the effect of matrix-to-reinforcement particle size ratio (PSR) on the particle dispersion and TC of Dia/Al composites by using starting Al powders with different size. The underlying cause of different particle

dispersion related to PSR was discussed. This study supplies a new idea to improve thermal conduction of Dia/Al composites with certain volume fraction of diamond particles by tuning particle dispersion, which is also applicable to other MMCs.

## Experimental

### Material preparation

A synthetic cubo-octahedron diamond powder (Type HWD40) of 70/80 mesh in size (180–210  $\mu\text{m}$ ) was used as the reinforcement particle, whose TC was estimated to be 1700–1850 W/mK according to the relationship between TC and nitrogen inclusion [11, 12]. Figure 1a, b shows the macroscopic and microscopic morphologies of diamond particles used in this study. Commercially atomized pure Al powders of 60/80, 120/140, 200/230 and 325/400 mesh in size were used as the matrix, as shown in Fig. 1c–f, whose nominal purity was 99.9%, with the tested value over 99.84% by inductively coupled plasma mass spectrometer (ICP-MS) [11, 32]. The oxygen contents in the as-received pure Al powders of various sizes were measured by an ONH836 Oxygen/Nitrogen/Hydrogen Elemental Analyzer (Leco Corporation, USA), to consider the effect of oxide skin naturally born on Al powders on the TC of the bulk Dia/Al composites. The oxygen contents were tested ranging of 1500–2000 ppm, which indicated a very little variation for different powder sizes and practicable to used as the matrix.

The as-received diamond particles were first ultrasonicated in distilled water to eliminate impurities on their surfaces and then after being dried were directly mixed for 4 h with pure Al powders with PSR from 0.225 to 0.90 (accordingly designated as PSR0.225, PSR0.375, PSR0.6 and PSR0.9, respectively). The mixing process was completed in a laboratory jar mill using a sealable jar of 250 mL in volume, with the powder mixtures of 20 g and agate grinding balls of 100 g (a ratio of 3:5 for grinding balls in diameters of 5 and 10 mm, respectively). The powder mixtures were cold pressed into green compacts of disks of 10 mm in diameter and 3 mm in thickness and then sintered at 650  $^{\circ}\text{C}$  for 90 min under a uniaxial pressure of 67 MPa by vacuum hot pressing in a graphite mold. During the whole sintering process, the vacuum less than 0.005 Pa was maintained in the furnace [11, 32].

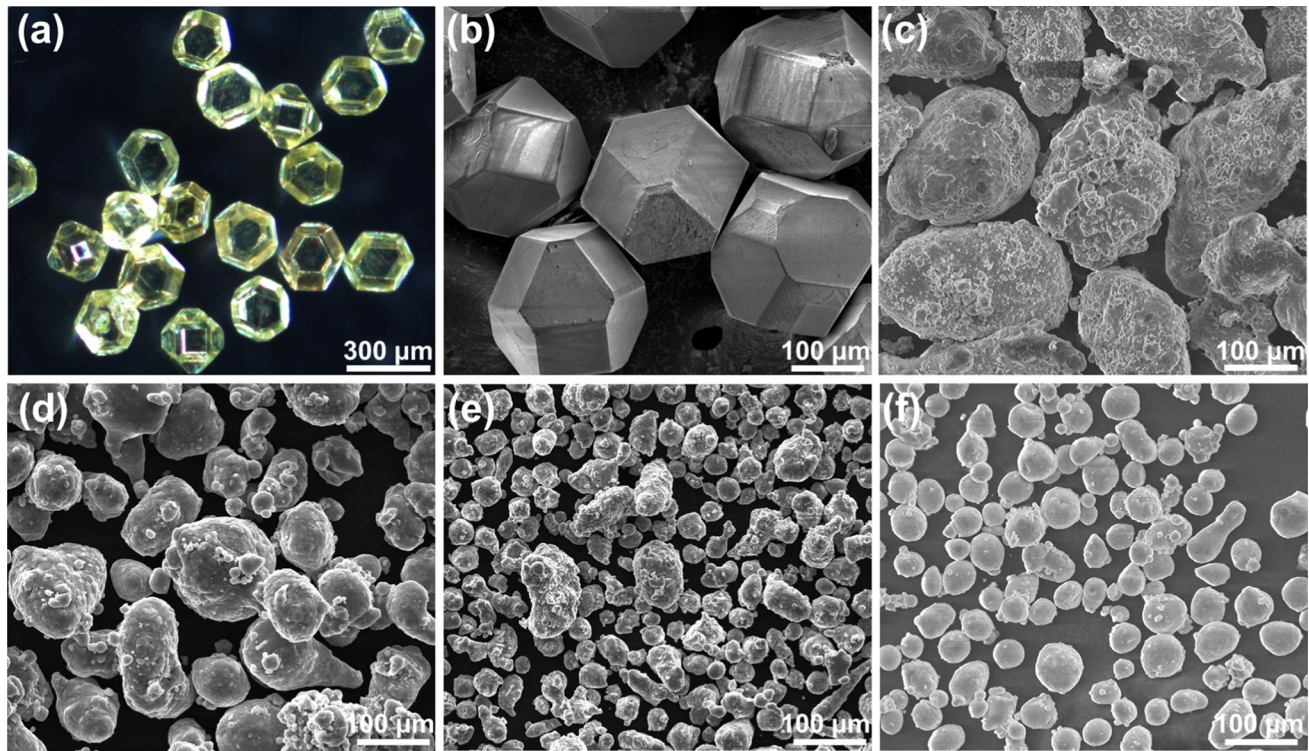


**Figure 1** Morphologies of the starting materials used in this study: **a** OM image of diamond particles of 70/80 mesh in size; **b** SEM images of the faceted diamond particles; **c–f** the as-atomized Al powders of **c** 60/80; **d** 120/140; **e** 200/230; **f** 325/400 mesh in size.

## Testing and characterizations

Thermal diffusivity of the vacuum hot pressed specimens was measured by laser flash technique using a Netzsch LFA447 thermal constant analyzer following the ASTM E-1461 International Standard. Each value represented an average of three measurements in all cases, and the standard deviation is 2%. The density of the sintered specimens was measured by the Archimedes method with a deviation below 1% for three repeated measurements, and the relative density was calculated by the ratio of the measured density to the theoretical density. Both the theoretical density and specific heat capacity were calculated by the rule of mixtures (ROM) based on the fraction of each component. TC of the sintered specimens was calculated by the product of the density, thermal diffusivity and specific heat capacity [7], and the uncertainty was supposed to be lower than  $\pm 3\%$ .

The morphologies of raw diamond particles and surfaces of Dia/Al green compacts were observed by optical microscopy (OM) using a KEYENCE VHX-1000E instrument. The morphologies of Al powders and fracture surfaces of the sintered specimens were

further examined by scanning electron microscopy (SEM) using an FEI Quanta FEG 250 instrument, operated at 20 kV. Due to the difficulty in treating stiff diamond particles, synchrotron radiation computed tomography (CT) of the sintered bulk composites was conducted at 40 keV using a detector of 9  $\mu\text{m}$  with a resolution of 18  $\mu\text{m}$ , on the beamline BL13W1 in Shanghai Synchrotron Radiation Facility (SSRF), China. This supplies a nondestructive manner to determine the spatial distribution of diamond particles in the Dia/Al composites. Some sectional views, named by sequential testing number of computed tomography (CT No.), were randomly taken for a direct observation of the diamond particles dispersion.

## Results

### Particle dispersion in the Dia/Al composites

Figure 2 shows the typical dispersion variation of diamond particles in 40 vol.% Dia/Al green compacts prepared by powder mixtures with different PSR. With the PSR increasing from 0.225 to 0.9,

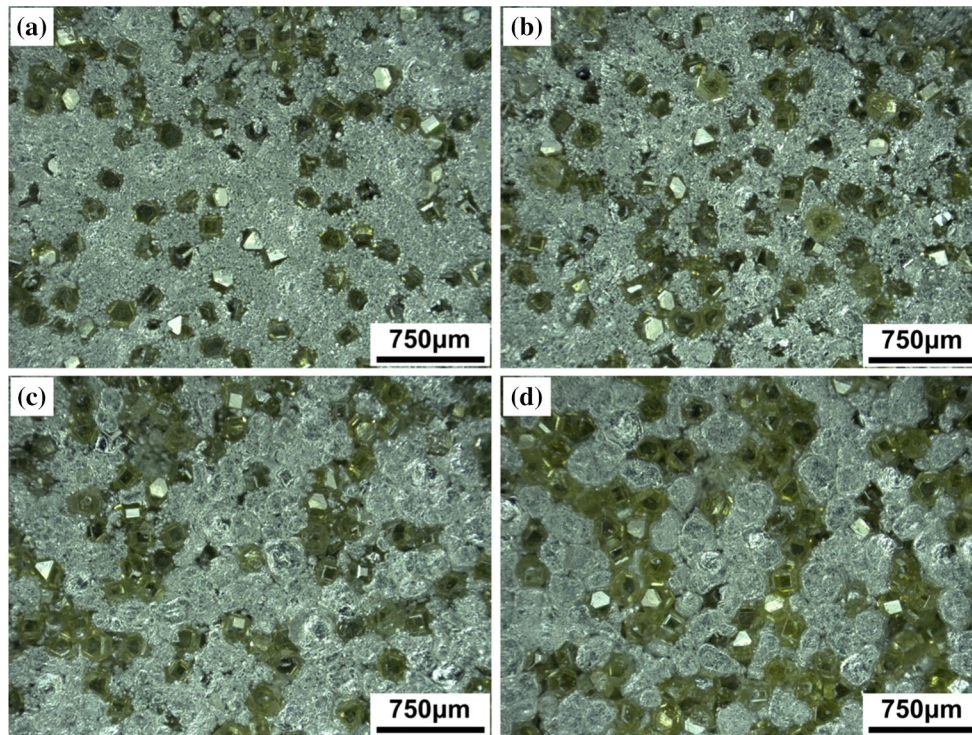


**Figure 2** OM morphologies of diamond particle dispersion in 40 vol.% Dia/Al green compacts of: **a** PSR0.225; **b** PSR0.375; **c** PSR0.6; **d** PSR0.9 powders.

diamond particles turned into connected groups from discrete particles. From the green compacts made of PSR0.225 powders, most diamond particles were randomly isolated by fine Al powders with some of them locally gathering (generally seemed as uniform dispersion). When PSR increased to 0.375, particles tended to connect with each other as connected groups containing 3–5 particles, but not connected as networks yet. However, when the PSR increased to 0.6 and 0.9, most particles formed continuous branches and an intercrossed network of diamond particles and coarse Al powders.

This different particle dispersion in the composites with different PSR can be further well retained after the solid sintering process of vacuum hot pressing, but the particle dispersion in the sintered Dia/Al composites can hardly be measured and observed by conventional characterizations. And it is even a rather challenging job to smoothly polish these composites, due to the stiffest feature of diamond particles and the contrasting properties of diamond and the Al matrix [33]. Alternatively, CT supplied by the synchrotron radiation facility can reveal the real dispersion of heterogeneous particles in metal matrix in a 3D space via a nondestructive manner. In this

study, to directly reveal the particle dispersion, several sectional views were randomly taken from the measured CT contour. Figures 3 and 4 are typical images randomly taken from CTs of the 40 vol.% Dia/Al composites prepared using powders of PSR0.225 and PSR0.9, respectively. As shown in Figure 3, diamond particles were uniformly dispersed in the PSR0.225 composites, with most particles isolated in the metal matrix (in light gray color). There was little difference in images taken from different layers of CT, revealing the real and popular status of particle dispersion in the sintered Dia/Al composites. In addition, some micropores were also present near the margin of the samples, as shown by the white arrows, which indicated that the consolidation of Dia/Al composites with homogeneously dispersed diamond particles was more difficult at the edge of samples, due to the poor mobility of the powder mixtures constrained by the wall of graphite mold during sintering.

Contrarily, diamond particles were distributed in a very uneven manner in the PSR0.9 composite, with several or tens of them tightly contacted with each other as branches or polygonal lines. Caused by this uneven particle dispersion, the consolidation of the

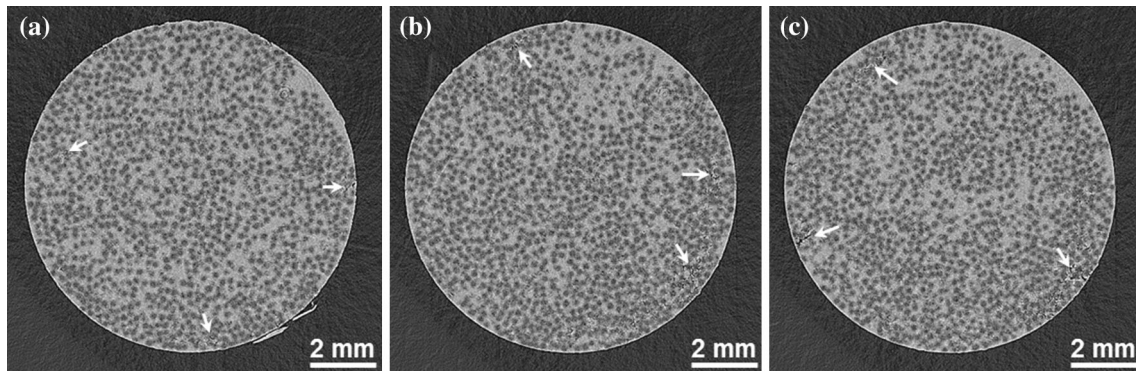


**Figure 3** CT images of the 40 vol.% Dia/Al composites of PSR0.225 powders. The white arrows show some micropores near the margin of the samples. CT No. **a** 150; **b** 300; **c** 400.

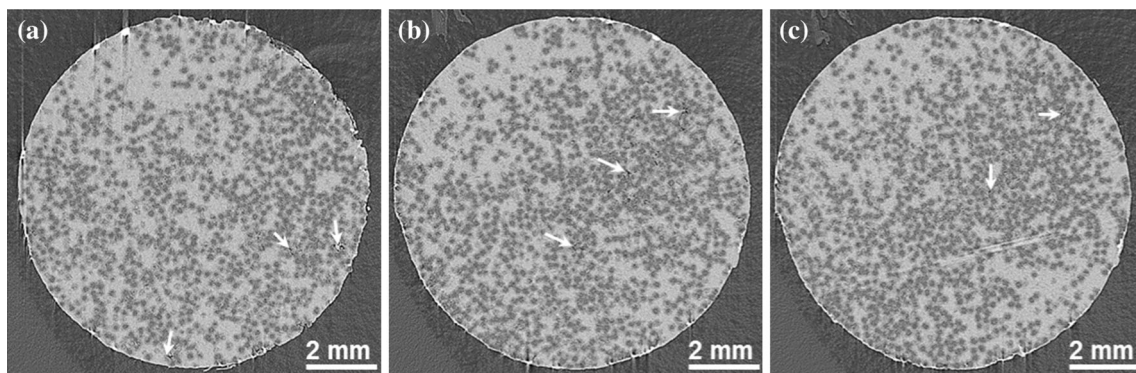


**Figure 4** CT images of the 40 vol.% Dia/Al composites of PSR0.9 powders. The white arrows show some micropores in the samples. CT No.: **a** 115; **b** 345; **c** 455.

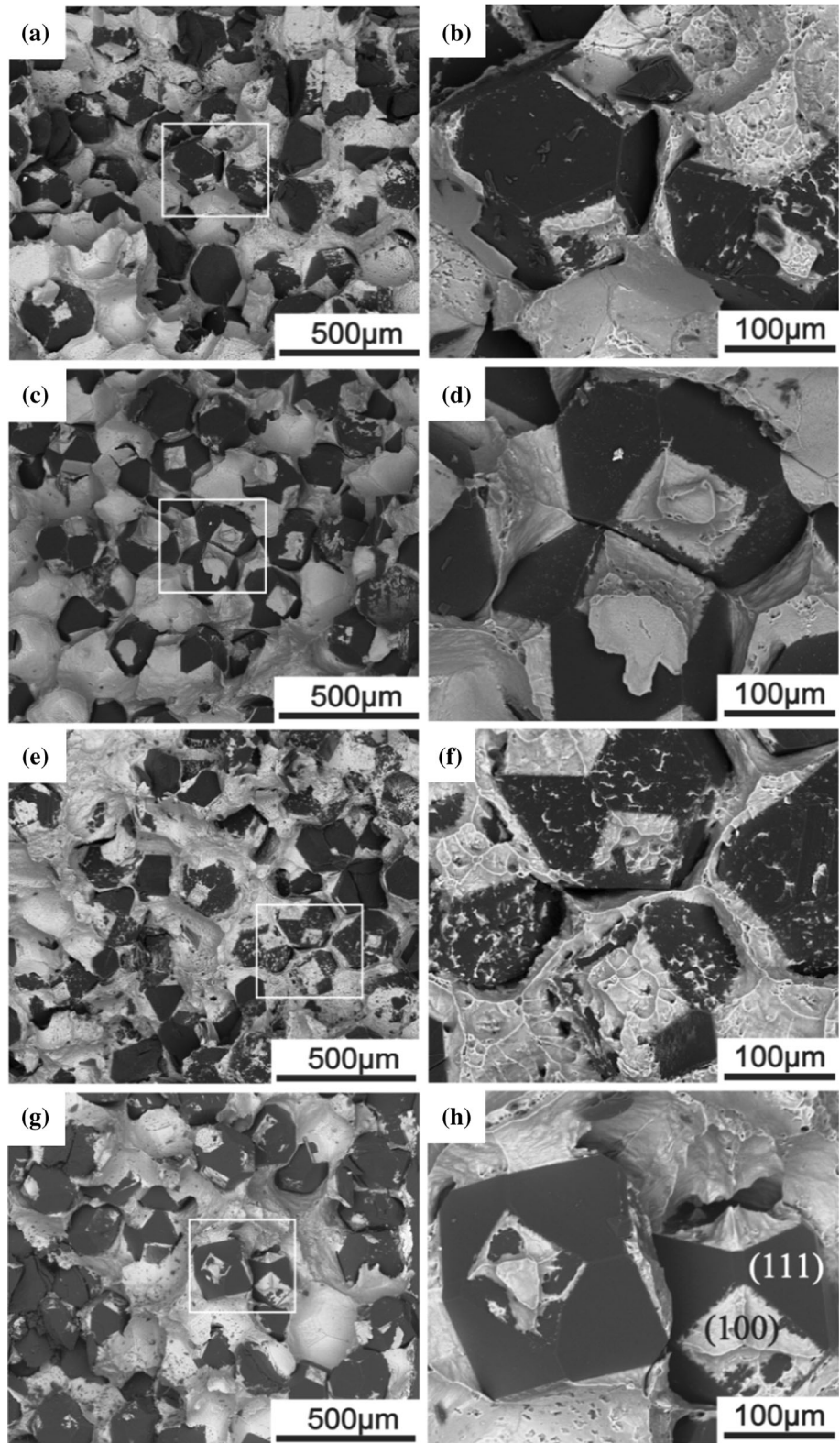
Dia/Al composite became more difficult compared to the PSR0.225 counterpart, with some pores observed both in the marginal and center areas in the sample, mainly present in the local area that particles clustered, as shown by the white arrows. It could be noted that the dispersion of diamond particles in the sintered composites observed by CT agreed well with the corresponding green compacts as observed in Fig. 2 by OM, i.e., with PSR increasing the particle dispersion turned to be more connected from isolated.

### Microstructure and interface of the Dia/Al composites

Figure 5 shows fracture surfaces of the 40 vol.% Dia/Al composites of different PSR sintered at 650 °C for 90 min, which shows a similar consolidation and interfacial bonding state. The plastic dimples on fracture surface indicate a ductile fracture mode of Al matrix. Good interfacial bonding is also revealed by

the plastic fractures of Al matrix rather than at the Dia/Al interface, with torn Al left on diamond {100} faces due to the preferred adherence of {100} faces originating from different carbon diffusion abilities on the {100} and {111} faces [11, 34]. Comparatively, in the PSR0.6 composite, the {111} faces also show a strong interfacial bonding as revealed by the presence of some adhered aluminum. But as characterized in the previous studies by XRD and HRTEM [11, 19], even in such a case of the PSR0.6 composite, there was very few interfacial reaction products found, i.e.,  $Al_4C_3$  compound, indicating very little difference present on the interfacial bonding state in between the PSR0.225, PSR0.375, PSR0.6 and PSR0.9 composites. More importantly, this also means that in such cases TC variation of these composites may mainly originate from the variation of the particle dispersion, rather than the marginal difference of the interfacial bonding state.

**Figure 5** SEM images showing fracture surfaces of the 40 vol.% Dia/Al composites of: **a, b** PSR0.225; **c, d** PSR0.375; **e, f** PSR0.6; **g, h** PSR0.9. **b, d, f, h** are zoom in images of the white frames in **a, c, e, g**, respectively.



## Thermal conductivity of the Dia/Al composites

Table 1 shows the physical property of the Dia/Al composites prepared by using the powder mixtures of different PSR. Figure 6a shows the relative density of the Dia/Al composites. With the volume fraction of diamond particles and PSR increasing, the relative density slightly decreased. Typically, with PSR increasing from 0.225 to 0.9, the relative density of the 40 vol.% Dia/Al composites decreased from 99.7 to 97.1%, which was in accordance with the increasing of pores in the sintered Dia/Al composites as shown by CT observations in Figs. 3 and 4. The relative density of 50 vol.% Dia/Al composites showed a similar variation, which decreased from 95.2 to

94.6%. In addition, with the volume fraction of diamond particles increasing from 40 to 50 vol.%, the relative density decreased from 97.7 to 95.2% for the PSR0.225 composites, and it decreased from 97.1 to 94.6% for the PSR0.9 counterparts. Thus, both increases in PSR and diamond content render the densification of the composites more difficult.

The TC of Dia/Al composites with various PSR is shown in Fig. 6b. The PSR tuning played an important role on the TC improvement of Dia/Al composites. With PSR increasing from 0.225 to 0.9, the TC of 40 vol.% Dia/Al composites increased by 21%, from 389 to 472 W/mK, while it increased even by 41% for 50 vol.% Dia/Al composites from 442 to 628 W/mK. To the best of our knowledge, the TC of 50 vol.% Dia/Al composites was very high compared

**Table 1** Physical property of the vacuum hot pressed Dia/Al composites

Diamond content (vol.%)	PSR	Density (g/cm <sup>3</sup> )	Theoretical density (g/cm <sup>3</sup> )	Relative density (%)	Thermal diffusivity (mm <sup>2</sup> /s)	Specific heat capacity (J/gK)	Thermal conductivity (W/mK)
40	0.225	2.958	3.028	97.69	183.4	0.717	389
	0.375	2.954		97.57	203.5		431
	0.6	2.941		97.13	211.5		446
	0.9	2.939		97.07	224.0		472
50	0.225	2.959	3.110	95.15	220.3	0.678	442
	0.375	2.910		93.58	231.1		456
	0.6	2.972		95.55	277.9		560
	0.9	2.943		94.62	314.7		628

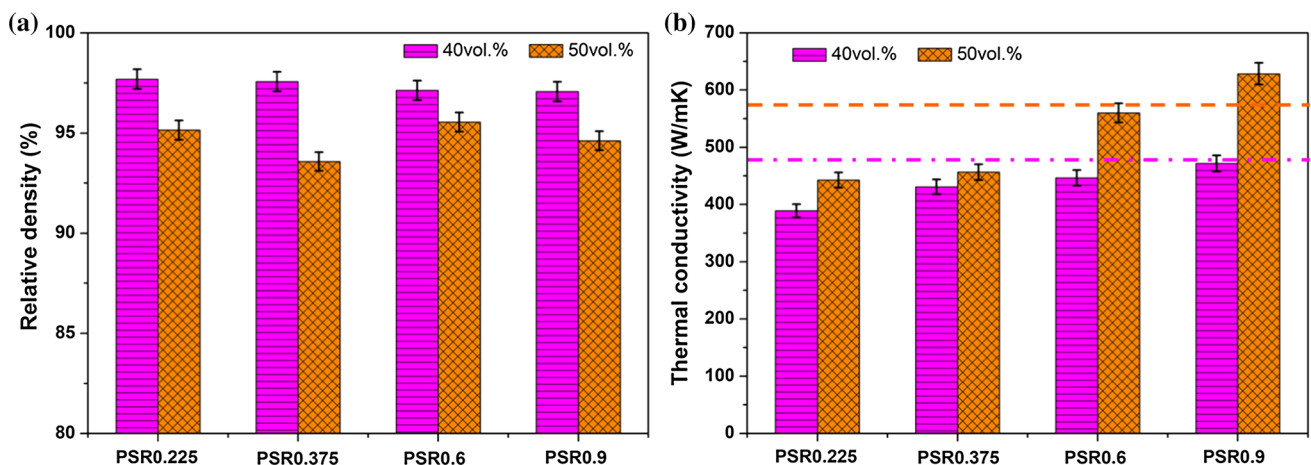


**Figure 6** **a** Relative density and **b** thermal conductivity of the 40 and 50 vol.% Dia/Al composites prepared by using powders with different PSR. The dash and dot-dash lines in **b** show the predicted

values of 40 and 50 vol.% Dia/Al composites by differential effective medium.

**Table 2** Physical property of the vacuum hot pressed pure Al

Size (mesh)	Density (g/cm <sup>3</sup> )	Theoretical density (g/cm <sup>3</sup> )	Relative density (%)	Thermal diffusivity (mm <sup>2</sup> /s)	Specific heat capacity (J/gK)	Thermal conductivity (W/mK)
60/80	2.667	2.70	98.78	91.4	0.895	218
120/140	2.698		99.93	92.7		224
200/230	2.688		99.56	92.0		221
325/400	2.683		99.37	92.5		222

with those from references [26, 27]. For comparison, the physical property of pure Al matrix made of different powder sizes is also listed in Table 2. There was no clear variation of the TC for all the pure Al samples ranging of 218–224 W/mK with an uncertainty of ± 7 W/mK. These equivalent values can be explained by the same level of impurity and oxygen contents in pure Al powders, which means the same chemical composition and TC of the matrix in Dia/Al composites with different PSR. Therefore, considering the same level of the TC of pure Al matrix and interfacial bonding of Dia/Al, the TC enhancement of Dia/Al composites was greatly influenced by the particle dispersion via PSR.

### Discussions

The TC of Dia/Al composites can be evaluated by the differential effective medium (DEM) scheme, which is effective for TC prediction for the composites with a high phase contrast [35, 36]:

$$(1 - V_r) \left( \frac{K_c}{K_m} \right)^{\frac{1}{3}} = \frac{K_r^{eff} - K_c}{K_r^{eff} - K_m} \tag{1}$$

where  $K_c$ ,  $K_m$  and  $V_r$  are the TC of the composites, the TC of the metal matrix and the volume fraction of reinforcement, respectively.  $K_r^{eff}$  is the effective TC of reinforcements by considering the interface conductance and the size of reinforcements, and can be expressed by Eq. (2) [37]:

$$K_r^{eff} = \frac{K_r^{in}}{1 + \frac{K_r^{in}}{h_c a}} \tag{2}$$

where  $K_r^{in}$ ,  $a$  and  $h_c$  are the intrinsic TC, the average radius of reinforcements and the interface conductance, respectively. The intrinsic TC of diamond particles used in this study was previously evaluated in the range of 1700–1850 W/mK [11], and here a

moderate value of 1800 W/mK was used for the theoretical calculation of TC. For the interface conductance,  $h_c$ , it was directly measured as  $5 \times 10^7$  W/m<sup>2</sup>K for diamond/Al system in experiments [38], which was also very close with the calculated value of  $4.63 \times 10^7$  W/m<sup>2</sup>K [39], and thus  $5 \times 10^7$  W/m<sup>2</sup>K was used for the theoretical calculation.

When the porosity of the composites is considered, the residual pores, supposed to be mainly present in the metal matrix as nonthermally conducting inclusions, contribute to constitute an effective metal matrix that has an effective TC,  $K_m^{eff}$ , expressed as [37]:

$$K_m^{eff} = K_m^{in} \frac{1 - V_p}{1 + 0.5V_p} \tag{3}$$

where  $V_p$  is the measured porosity in the composites, and  $K_m^{in}$  is the intrinsic TC of the metal matrix (free of pores). Specially, the pure Al matrix (99.84% in purity) sintered at 650 °C for 90 min has a relative density of 98.78–99.93% and  $K_m^{eff}$  of 218–224 W/mK; thus, the  $K_m^{in}$  back concluded by Eq. (2), is 222–224 W/mK [11].

For 40 and 50 vol.% Dia/Al composites, the measured TC increased with the PSR increasing. The measured TC of 40 vol.% Dia/Al composites increased from 82 to 99% of the prediction by DEM with PSR increasing from 0.225 to 0.9. On the other hand, the measured TC of 50 vol.% Dia/Al composites increased from 77.6 to 98% with PSR increasing from 0.225 to 0.6, and even reached 110% of the prediction by DEM for the PSR0.9 composites, which was not reported so far. This TC variation between experiment and prediction may originate from the assumption that particles were uniformly dispersed in matrix and the effect between neighboring particles can be totally ignored [35, 40]. However, in this study, diamond particles dispersed as connected groups in the PSR0.9 composite, where the effect between neighboring particles was serious, probably



analogized as connected dispersion of metallic inclusions in insulator matrix.

The role of PSR on the particle dispersion can be explained by the variation of the coordination number of Al powders around diamond particles. For certain size and volume fraction of diamond particles, there are much more Al powders in the powder mixtures for a smaller PSR, i.e., smaller and more Al powders; thus, a larger coordination number of Al powders around each diamond particle is expected. In this way, with too many fine Al powders surrounded, diamond particles are more likely to be separated from each other. In contrast, in a powder mixture of large PSR, i.e., larger and fewer Al powders will lead to a lower coordination number, which is insufficient to isolate the contact and connection of diamond particles.

It was supposed that when a single size of reinforcement and metal powders were used, with the number of metal powders no less than that of the reinforcement particles, similar sizes (i.e., PSR close to 1) of metal powders and reinforcement particles are preferred to balance the agglomeration of reinforcement particles and the consolidation of the metal matrix as well as a desirable particle dispersion. Specially, for the Dia/Al composites with a higher volume of diamond particles, the increase in PSR will inevitably lead to a drastic decrease in the number of Al powders (fewer than that of diamond particles), which made the interstices in between neighboring diamond particles no longer filled by Al powders, and thus, the severe agglomeration of diamond particles posed great difficulty to the consolidation of composite, considering that neighboring diamond particles cannot be sintered together and thus leading to a large heat barrier. Consequently, TC of the composites with a higher volume of diamond particles will decline drastically.

Although the effect of PSR on diamond particle dispersion and further on the TC of the Dia/Al composites was revealed to some extent by experimental results, the intrinsic and physical principle of the TC improvement was still an open topic, and much more work needs to be done in the future. It is not expected that the diamond simply builds solid bridges among their particles, but probably correlating with the mean free path of phonons in connected diamond particles when transmitting heat/energy at interface. The variation of reinforcement size, shape and thermal property may also be relevant to its

dispersion, especially to the phonon transmission between neighboring surfaces of the connected diamond particles, and thus influence the TC of the bulk materials. Clearly, this study is also applicable to other MMCs prepared by PM, e.g., Dia/Cu, Dia/Ag and SiCp/Al (or Cu) composites.

## Conclusions

This study supplies a new idea to improve thermal conductivity of Dia/Al composites with certain volume fraction of diamond particles by tuning particle dispersion. 40–50 vol.% Dia/Al composites were fabricated by powder metallurgy using Al powders of different size to adjust the matrix-to-reinforcement particle size ratio (PSR) and particle dispersion. The optical microscopy of the green compacts and synchrotron radiation CT of the sintered samples revealed diamond particles tend to form connecting dispersion with PSR increasing. The thermal conductivity of 40 and 50 vol.% Dia/Al composites increased by 21% (from 389 to 472 W/mK) and 42% (from 442 to 628 W/mK), respectively, with PSR increasing from 0.225 to 0.9. But the intrinsic and physical principle of the thermal conductivity improvement of Dia/Al composites via tuning PSR is still unclear and to be revealed in the future.

## Acknowledgements

The authors would like to acknowledge the financial support of the National Natural Science Foundation (Nos. 51401123, 51371115, 51671130), the Ministry of Science & Technology of China (No. 2017YFB0406200), the 111 Project (Grant No. B16032), and Shanghai Science & Technology Committee (Nos. 15JC1402100, 17ZR1441500, 14DZ2261200, 14520710100). Dr. Z. Tan thanks to the Project funded by the China Postdoctoral Science Foundation (No. 2014M561469). And all the authors acknowledge the Shanghai Synchrotron Radiation Facility (SSRF) for the analysis of synchrotron radiation CT of the metal matrix composites.

## References

- [1] Zweben C (2008) Advances in photonics thermal management and packaging materials. *Proc Soc Photo-Opt Inst* 6899:689918–6899181
- [2] Qu XH, Zhang L, Wu M, Ren SB (2011) Review of metal matrix composites with high thermal conductivity for thermal management applications. *Prog Nat Sci* 21:189–197
- [3] Moore AL, Shi L (2014) Emerging challenges and materials for thermal management of electronics. *Mater Today* 17:163–174
- [4] Arpón R, Molina JM, Saravanan RA, García-Cordovilla C, Louis E, Narciso J (2003) Thermal expansion behaviour of aluminium/SiC composites with bimodal particle distributions. *Acta Mater* 51:3145–3156
- [5] Molina-Jordá JM (2015) Nano- and micro-/meso-scale engineered magnesium/diamond composites: novel materials for emerging challenges in thermal management. *Acta Mater* 96:101–110
- [6] Schobel M, Degischer HP, Vaucher S, Hofmann M, Cloetens P (2010) Reinforcement architectures and thermal fatigue in diamond particle-reinforced aluminum. *Acta Mater* 58:6421–6430
- [7] Kidalov SV, Shakhov FM (2009) Thermal conductivity of diamond composites. *Materials* 2:2467–2495
- [8] Monje IE, Louis E, Molina JM (2016) Role of  $Al_4C_3$  on the stability of the thermal conductivity of Al/diamond composites subjected to constant or oscillating temperature in a humid environment. *J Mater Sci* 51:1–10. <https://doi.org/10.1007/s10853-016-0072-8>
- [9] Molina-Jorda JM (2015) Design of composites for thermal management: aluminum reinforced with diamond-containing bimodal particle mixtures. *Compos Part A* 70:45–51
- [10] Chen H, Jia CC, Li SJ (2012) Interfacial characterization and thermal conductivity of diamond/Cu composites prepared by two HPHT techniques. *J Mater Sci* 47:3367–3375. <https://doi.org/10.1007/s10853-011-6180-6>
- [11] Tan ZQ, Li ZQ, Fan GL, Kai XZ, Ji G, Zhang LT et al (2013) Fabrication of diamond/aluminum composites by vacuum hot pressing: process optimization and thermal properties. *Compos Part B* 47:173–180
- [12] Yamamoto Y, Imai T, Tanabe K, Tsuno T, Kumazawa Y, Fujimori N (1997) The measurement of thermal properties of diamond. *Diam Relat Mater* 6:1057–1061
- [13] Flaquer J, Rios A, Martin-Meizoso A, Nogales S, Bohm H (2007) Effect of diamond shapes and associated thermal boundary resistance on thermal conductivity of diamond-based composites. *Comp Mater Sci* 41:156–163
- [14] Molina JM, Saravanan RA, Arpon R, Garcia-Cordovilla C, Louis E, Narciso J (2002) Pressure infiltration of liquid aluminium into packed SiC particulate with a bimodal size distribution. *Acta Mater* 50:247–257
- [15] Zhang Y, Li J, Zhao L, Wang X (2015) Optimisation of high thermal conductivity Al/diamond composites produced by gas pressure infiltration by controlling infiltration temperature and pressure. *J Mater Sci* 50:688–696. <https://doi.org/10.1007/s10853-014-8628-y>
- [16] Weber L, Tavangar R (2009) Diamond-based metal matrix composites for thermal management made by liquid metal infiltration-potential and limits. *Adv Mater Res* 59:111–115
- [17] Tan ZQ, Li ZQ, Xiong DB, Fan GL, Ji G, Zhang D (2014) A predictive model for interfacial thermal conductance in surface metallized diamond aluminum matrix composites. *Mater Des* 55:257–262
- [18] Monje IE, Louis E, Molina JM (2013) Optimizing thermal conductivity in gas-pressure infiltrated aluminum/diamond composites by precise processing control. *Compos Part A* 48:9–14
- [19] Tan Z, Ji G, Addad A, Li Z, Silvain J-F, Zhang D (2016) Tailoring interfacial bonding states of highly thermal performance diamond/Al composites: spark plasma sintering versus vacuum hot pressing. *Compos A* 91:9–19
- [20] Monje IE, Louis E, Molina JM (2016) Interfacial nano-engineering in Al/diamond composites for thermal management by in situ diamond surface gas desorption. *Scr Mater* 115:159–163
- [21] Feng H, Yu JK, Tan W (2010) Microstructure and thermal properties of diamond/aluminum composites with TiC coating on diamond particles. *Mater Chem Phys* 124:851–855
- [22] Tan ZQ, Li ZQ, Fan GL, Guo Q, Kai XZ, Ji G et al (2013) Enhanced thermal conductivity in diamond/aluminum composites with a tungsten interface nanolayer. *Mater Des* 47:160–166
- [23] Weber L, Tavangar R (2007) On the influence of active element content on the thermal conductivity and thermal expansion of Cu–X (X=Cr, B) diamond composites. *Scr Mater* 57:988–991
- [24] Zhang H, Wu J, Zhang Y, Li J, Wang X, Sun Y (2015) Mechanical properties of diamond/Al composites with Ti-coated diamond particles produced by gas-assisted pressure infiltration. *Mater Sci Eng A* 626:362–368
- [25] Xue C, Yu JK (2013) Enhanced thermal conductivity in diamond/aluminum composites: comparison between the methods of adding Ti into Al matrix and coating Ti onto diamond surface. *Surf Coat Tech* 217:46–50
- [26] Yang W, Chen G, Wang P, Qiao J, Hu F, Liu S et al (2017) Enhanced thermal conductivity in Diamond/Aluminum composites with tungsten coatings on diamond particles

- prepared by magnetron sputtering method. *J Alloy Compd* 726:623–631
- [27] Che Z, Wang Q, Wang L, Li J, Zhang H, Zhang Y et al (2017) Interfacial structure evolution of Ti-coated diamond particle reinforced Al matrix composite produced by gas pressure infiltration. *Compos B* 113:285–290
- [28] Li Z, Tan Z, Fan G, Zhang D (2013) Progress of metal matrix composites for efficient thermal management applications. *Mater China* 32:431–440
- [29] Ashby M (2013) Designing architected materials. *Scr Mater* 68:4–7
- [30] Kusy R (1977) Influence of particle size ratio on the continuity of aggregates. *J Appl Phys* 48:5301–5305
- [31] Zhang Y, Zhang HL, Wu JH, Wang XT (2011) Enhanced thermal conductivity in copper matrix composites reinforced with titanium-coated diamond particles. *Scr Mater* 65:1097–1100
- [32] Tan ZQ, Li ZQ, Fan GL, Kai XZ, Ji G, Zhang LT et al (2013) Diamond/aluminum composites processed by vacuum hot pressing: microstructure characteristics and thermal properties. *Diam Relat Mater* 31:1–5
- [33] Ji G, Tan ZQ, Shabadi R, Li ZQ, Grunewald W, Addad A et al (2014) Triple ion beam cutting of diamond/Al composites for interface characterization. *Mater Charact* 89:132–137
- [34] Kleiner S, Khalid FA, Ruch PW, Meier S, Beffort O (2006) Effect of diamond crystallographic orientation on dissolution and carbide formation in contact with liquid aluminium. *Scr Mater* 55:291–294
- [35] Bruggeman DAG (1935) The prediction of the thermal conductivity of heterogeneous mixtures. *Ann Phys* 24:636–664
- [36] Tavangar R, Molina JM, Weber L (2007) Assessing predictive schemes for thermal conductivity against diamond-reinforced silver matrix composites at intermediate phase contrast. *Scr Mater* 56:357–360
- [37] Molina JM, Prieto R, Narciso J, Louis E (2009) The effect of porosity on the thermal conductivity of Al-12 wt% Si/SiC composites. *Scr Mater* 60:582–585
- [38] Stoner R, Maris H, Anthony T, Banholzer W (1992) Measurements of the Kapitza conductance between diamond and several metals. *Phys Rev Lett* 68:1563–1566
- [39] Caccia M, Rodriguez A, Narciso J (2014) Diamond surface modification to enhance interfacial thermal conductivity in Al/diamond composites. *JOM* 66:920–925
- [40] Molina JM, Narciso J, Weber L, Mortensen A, Louis E (2008) Thermal conductivity of Al–SiC composites with monomodal and bimodal particle size distribution. *Mater Sci Eng A* 480:483–488